The effect of shrinkage on the cooking of meat

A. J. Fowler and A. Bejan
Department of Mechanical Engineering and Materials Science, Duke University, Durham, NC, USA

In this paper the cooking of meat is modeled as a process of time-dependent conduction through a constant-property medium that shrinks as its temperature increases. The overall shrinkage is the integrated result of shrinking that is distributed volumetrically through the piece of meat and depends on the temperature history at every point. The meat temperature history and associated shrinkage are determined numerically. The geometric configuration is the one-dimensional conducting slab with convective heating on both sides. Means for calculating the required cooking time are reported in the form of dimensionless charts for the temperature in the midplane of the meat slab. A numerical example shows that the cooking time calculated by accounting for meat shrinkage is appreciably shorter than the time estimate based on the classical Heisler chart for conduction in a constant-volume slab.

Keywords: food technology; conduction; materials processing

Background

The previous efforts to develop models for the cooking of meat fall into two basic groups, labeled A and B in this discussion. In the first group are those that approach the problem by looking at very specific food products and attempt to develop accurate models for cooking those products in specific environments. The advantage of this method is that it accounts for special features in the cooking process, features that are unusual or even unique to the food that is modeled.

The second group of studies focuses on specific aspects of the cooking process in order to develop general guidelines for cooking models of all types. Since the reactions that take place when cooking meat are numerous and complex, it is extremely useful to analyze those reactions specifically in order to identify the ones that can be ignored and the ones that can be subjected to simplifying assumptions.

Group A

The leading example of research of the first kind is the work of Holtz and Skjöldebrand,[1-3] who looked exclusively at minced meat loaves being cooked in forced convection ovens. They begin with purely experimental work. In an early paper by Skjöldebrand[1] the mass and heat transfer coefficients for the process were determined experimentally. In another experimental paper, Holtz and Skjöldebrand[2] found relationships between weight loss and the formation of a crust at the meat loaf surface, and the relation between "sensorial aspects" and oven conditions. Using all of these empirically determined relationships they developed a complete mathematical model for the cooking of meat loaf in a forced convection oven.[3] The mathematical model takes into account heat and mass transfer, crust formation, and the evaporation of water at the crust–crumb interface (where the dry crust surface touches the moist interior of the meat loaf).

Address reprint requests to Professor Bejan at the Department of Mechanical Engineering and Materials Science, Duke University, Durham, NC 27706, USA.

Received 13 March 1991; accepted 13 May 1991

The ability of Holtz and Skjöldebrand's model to predict the actual cooking time is characterized by an error of 15–30 percent, depending on the cooking conditions. They attributed this error to the uncertainty in the specified value for the thermal diffusivity of meat, to the neglect of the effects of meat quality and water-holding ingredients, and above all, to the neglect of meat shrinkage during cooking.

Another fairly complete model for the cooking of a specific meat product (boiled shrimp) was developed by Chau and Snyder.[4] They determined experimentally the heat transfer coefficient and the thermal properties of shrimp and solved numerically the heat conduction problem in a simplified geometry that approximated the shape of a shrimp. Although their model predicted well the centerline temperature during cooking, they did find that some error accumulated near the end of the process.

Most interesting is that Chau and Snyder wanted to be able to also predict the cooling of the cooked shrimp for storage, and that their model had large errors in the prediction of the temperature history during cooling. Experimentally, they showed that the shrimp had become appreciably smaller after cooking. Their model was subsequently improved by adjusting the shrimp to a new (smaller) size when the model shifted from the cooking mode to the cooling mode.

Bengtsson et al.[5] studied oven-roasted beef. Like Holtz and Skjöldebrand, they considered many factors in the cooking process—heat and mass transfer, weight loss, and moisture and fat content—and developed a fairly simple model for temperature prediction. In the end they found that their model worked fairly well in the early stages of cooking, but began to overestimate the temperature in the meat as time progressed. They attributed this error to the possible swelling of the meat. This explanation, however, is questionable: it seems unlikely that the error was a result of meat swelling, as every other researcher has found that meat shrinks rather than swells during cooking.

Dagerskog[6] published two related articles analyzing the frying of hamburger patties. He analyzed weight loss, crust formation, heat transfer, and particularly mass transfer. By inserting a plastic barrier between layers of a hamburger patty, he showed, both experimentally and numerically, that mass

transfer inside the patty increases heat penetration. His numerical model was fairly accurate in predicting temperature distribution and water loss.

The major drawback of all these models is their heavy dependence on empirical data, which are specific to the cuts of meat being cooked and the manner in which the cooking takes place. The functions for the heat transfer coefficients are all determined empirically without any attempt to indicate under what conditions similar heat transfer coefficient values might be valid. The models for crust formation, and moisture release are similarly dependent on the specific cuts of meat. Meat shrinkage, or swelling, is acknowledged as a cause for error, but no attempt is made to actually model the shrinkage of meat as cooking progresses, or to explore how large an error might result from neglecting this effect.

Group B

In the second group, the most general meat-cooking study to date has been performed by Burfoot and James.[7,8] In their 1984 paper they made an analytical estimate for the heat transfer coefficient for combined convection and radiation. They also investigated experimentally the degree of meat shrinkage (in a roughly cylindrical cut of meat) and found that the change in length between points in the meat varied from 4–46 percent after cooking. They found the overall longitudinal shrinkage was 20 percent. They incorporated this into their simple model by assuming that the radius of the meat cylinder decreased by 10 percent at the onset of cooking and then remained constant.

Burfoot and James[7] concluded that there are five important areas that need to be explored more thoroughly before an accurate and general cooking model can be developed: the values of the heat and mass transfer coefficients, the thermal properties of meat at high temperatures, the rate of diffusion, and the shrinkage. The latter forms the subject of the present study.

In a subsequent paper Burfoot and James[8] explored the variations in the heat transfer coefficient (h) and their effect on cooking and thawing times for cylindrical cuts of meat. They reported that the spatial variation in heat transfer coefficient made a large difference in cooking (h varied linearly along a meat cylinder oriented horizontally; it varied from the end to the midplane of the cylinder). They also found, however, that temporal variation of the heat transfer coefficient did not result in expected cooking times that were significantly different from those predicted using a time-averaged h. Trying to determine a time-dependent function of h, therefore, is a needless complication when developing a cooking model.

Hamm[9] examined experimentally the changes in the water-holding capacity of beef during cooking. The water-holding capacity is the beef's ability to resist the removal of liquid that could result from squeezing the beef or from gravity. Hamm found that beef loses a large portion of its water-holding capacity between 40 and 50°C. At temperatures greater than 50°C the water in beef begins to drip out under the influence of gravity and can be squeezed out by internal or uneven external pressure.

This result allowed Hung[10] to identify the mechanism for meat shrinkage during cooking. By using transmission electron microscopy in beef muscle he found that the shrinkage was the result of shrinking of the sarcomeres. Sarcomeres are units of the myofibril, which make up the muscle fibers. He found, moreover, that the sarcomere shrinkage was dependent almost exclusively on temperature rather than time of exposure to a given temperature. The shrinkage occurred in two phases; the first at a fairly low temperature and the second at a much higher temperature (70°C). Hung found experimentally that the first phase of sarcomere shrinkage did not result in weight loss or in dripping. The second phase, on the other hand, corresponded exactly with the major period of meat dripping. The change in the water-holding capacity that had been identified by Hamm allowed Hung to explain the difference in behavior between the two periods of sarcomere shrinkage.

Godslave et al.[11,12] conducted experiments in which they examined in detail the loss of moisture from beef during cooking and identified several stages in the dripping and drying process. In his thesis, Godslave[12] reported a model for temperature prediction when cooking beef; however, the model is based entirely on empirically determined constants (it is actually a curve fit of the experimental data).

In summary, the research of the second kind attempts to clarify specific aspects of the cooking process. Although the experiments involve specific cuts of meat, their results are fundamental enough to be incorporated in more general models.

Physical model

The objective of our work is to show the effect that the shrinking has on the cooking times of various cuts of meat. Meat consists primarily of liquid held in a protein matrix much like a sponge. At room temperature, however, the meat retains its liquid, so

Notation

Bi	Biot number, Equation 17
f	Shrinkage factor, Equation 6
f_∞	Final shrinkage factor, Figure 3
h	Heat transfer coefficient
k	Thermal conductivity of meat
L	Instantaneous half-thickness, Figure 1
L_0	Initial half-thickness, Figure 1
N	Number of parallel slices, Figure 1
t	Time
T	Temperature
T_c	Temperature in the midplane, $x = 0$, Figure 1
T_0	Initial temperature
T_1	Temperature at which shrinking begins
T_2	Temperature at which shrinking ends
T_∞	Ambient (oven) temperature
x	Transversal coordinate, Figure 1

Greek symbols

Δx	Instantaneous thickness of one slice
Δx_0	Initial thickness of one slice
α	Thermal diffusivity of meat
θ	Dimensionless temperature, Equation 15
θ_c	Dimensionless midplane temperature
θ_1	Dimensionless temperature at which shrinking begins, Figure 3
θ_2	Dimensionless temperature at which shrinking ends, Figure 3
λ	Dimensionless instantaneous half-thickness, Equation 16
ξ	Dimensionless transversal position, Equation 15
τ	Dimensionless time (Fourier number), Equation 16

that even under an uneven pressure distribution the liquid is not squeezed out. Hamm[9] showed that the water-holding capacity of meat decreases as cooking progresses, and that this decrease is almost complete when the meat temperature reaches approximately 60°C. He found that the water-holding capacity continues to decrease beyond the 60°C mark; however, the bulk of the decrease occurs in the 40–50°C range (see also McGree[13]). Beyond that range, the liquid can flow out of the protein matrix under the influence of gravity, or it can be squeezed out by applying pressure (e.g., with a spatula) in the same way that water can be squeezed out of a sponge.

In spite of the sizeable shrinkage exhibited during cooking, the density of meat remains nearly constant. This is because the cooking and shrinking is accompanied also by a loss of mass in the form of the liquid that is freed at the surface of the cut of meat. The liquid is pushed toward the surface by the protein matrix, which shrinks during cooking, and after reaching the surface it is removed by gravity.

In summary, the body of meat can be modeled as a conducting medium with constant density. The external surfaces of this body migrate toward the center as the cooking progresses. This model is used here only as a means of evaluating the magnitude of the heat transfer effect of meat shrinking, i.e., to decide if this effect is significant. It is worth mentioning that a more complete (predictive) model for meat cooking would incorporate the shrinking effect next to several other features that are currently left out (e.g., internal mass transfer, crust formation, surface evaporation).

Mathematical formulation

Consider the unidirectional conduction configuration defined in Figure 1. The piece of meat is modeled as a slab of initial half-thickness L_0 and initial temperature T_0. Beginning with the time $t = 0$, both sides of the slab are exposed to a fluid of temperature T_∞, across a constant heat transfer coefficient h. The slab material is stationary and homogeneous, and its

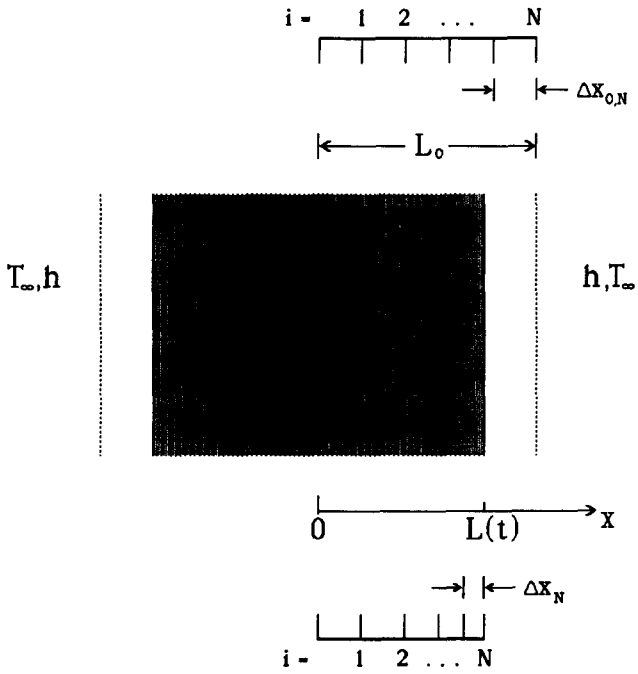

Figure 1 One-dimensional piece of meat (slab) with convective heat transfer and shrinkage

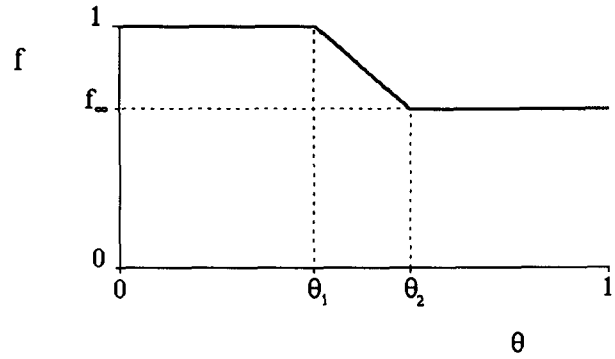

Figure 2 Piecewise linear model for the shrinkage factor f

thermal properties (k, α) are constant. In time, the local temperature $T(x, t)$ increases, and the associated shrinkage of the material is reflected in the monotonic decrease of the instantaneous half-thickness $L(t)$. The time-dependent conduction process is governed by the following equation, boundary conditions, and initial condition:

$$\frac{\partial T}{\partial t} = \alpha \frac{\partial^2 T}{\partial x^2} \tag{1}$$

$$\frac{\partial T}{\partial x} = 0, \quad \text{at} \quad x = 0 \tag{2}$$

$$k \frac{\partial T}{\partial x} = h(T_\infty - T), \quad \text{at} \quad x = L(t) \tag{3}$$

$$T = T_0 \quad \text{at} \quad t = 0 \tag{4}$$

What distinguishes this process from the classical problem of unsteady conduction in a slab[14] is the boundary condition (3) in which $L(t)$ is related to the history of the temperature distribution $T(x, t)$. In order to see the basis for this relationship, assume that the original half-thickness L_0 is divided into a large number (N) of slices of equal thickness (Figure 1, top).

$$\Delta x_0 = \frac{L_0}{N} \tag{5}$$

In time, each slice shrinks. In Figure 2 we will see that the shrinking of one slice (meat sample) is due to the elevated temperature of the sample. The instantaneous thickness of the i^{th} slice is related to the original thickness through the formula

$$\Delta x_i = \Delta x_0 f(T_i) \tag{6}$$

in which the shrinkage factor, f, is a known function of the slice temperature. (Note that $f \leq 1$). The instantaneous half-thickness of the slab is therefore

$$L(t) = \sum_{i=1}^{N} \Delta x_0 f[T_i(t)] \tag{7}$$

It is important to note that in this relation T_i is the temperature of the i^{th} slice, i.e., the temperature in a plane that moves toward $x = 0$ as the time, t, increases. In order to be able to use Equation 7, it is necessary to keep track of the movement (position) of each slice. We do this by calculating the instantaneous distance x_i between the slice (plane of temperature T_i) and the midplane of the slab.

$$x_i(t) = \sum_{j=1}^{i} \Delta x_0 f[T_j(t)] \tag{8}$$

In this way, the instantaneous positions of all the slices generate the curve labeled t in Figure 3. In the same figure, the initial

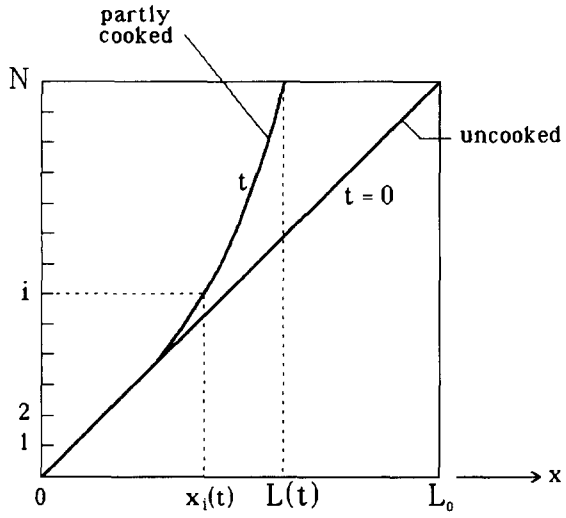

Figure 3 Shrinking curve, or the instantaneous position of each of the initial constant x planes in Figure 1 (top)

temperature distribution (the state of zero shrinkage) is represented by the straight line. The statement for the problem of determining the temperature distribution $T(x, t)$ becomes complete as we combine Equation 7 with the shrinkage curve of Figure 3:

$$L(t) = \sum_{i=1}^{N} \Delta x_0 f[T(x_i, t)] \tag{9}$$

It is convenient to restate Equations 1–4 and 9 in dimensionless terms:

$$\frac{\partial \theta}{\partial \tau} = \frac{\partial^2 \theta}{\partial \xi^2} \tag{10}$$

$$\frac{\partial \theta}{\partial \xi} = 0, \quad \text{at} \quad \xi = 0 \tag{11}$$

$$\frac{\partial \theta}{\partial \xi} = \text{Bi}(1 - \theta), \quad \text{at} \quad \xi = \lambda(\tau) \tag{12}$$

$$\theta = 0, \quad \text{at} \quad \tau = 0 \tag{13}$$

$$\lambda(\tau) = \frac{1}{N} \sum_{i=1}^{N} f[\theta(\xi_i, \tau)] \tag{14}$$

by defining the dimensionless variables

$$\theta = \frac{T - T_0}{T_\infty - T_0}, \qquad \xi = \frac{x}{L_0} \tag{15}$$

$$\tau = t \frac{\alpha}{L_0^2}, \qquad \lambda = \frac{L}{L_0} \tag{16}$$

The Biot number is based on the initial half-thickness

$$\text{Bi} = \frac{hL_0}{k} \tag{17}$$

Numerical method

The conduction Equation 10 was solved at each time step by using a solver based on the trapezoidal rule and the second-order accurate backward difference formula (TRBDF2). This solver is second-order accurate in both time and space. The number of grid points was 101; therefore, the global spatial error was on the order of one part in 10,000. The TRBDF2 solver is a composite method, which allows for an estimate of the local truncation error at each step. The time increment was chosen so as to force a local truncation error on the order of 10^{-3} of the norm of θ values at the gridpoints. The results of the TRBDF2 solver were verified by using a simple forward Euler solver; however, all the results exhibited in this paper were generated using the TRBDF2 solver.

The boundary conditions were implemented using the mirror point method. The values of the mirror points were determined by using second-order accurate slope discretizations. A zero slope boundary condition was used in the center of the slab and the exterior mirror point value was determined using a conduction–convection balance at the surface.

In order to account for the shrinking of the conduction domain, the L_0 slab was first divided into 100 equal slices. The initial dimensionless length of each slice was therefore 0.01. After the time step was advanced, the θ value at the midpoint of each slice was evaluated. Linear interpolation was used to determine the θ values at points that lay between gridpoints. The length of each of these segments was then adjusted using the shrinking model. The thicknesses of the slices were evaluated from the center to the surface, and then the new half-width of the slab was computed by adding up the thicknesses of all of the slices.

The θ grid had to be redrawn since the shrinkage leaves the exterior gridpoints beyond the edge of the slab. A new set of 101 evenly spaced gridpoints was drawn on the now thinner slab, and the θ at each gridpoint was determined using the old temperature profile. This resulted in a new θ profile that was a "truncated" version of the earlier profile, because the near-surface (hottest) material is forced out of the system as the plane $x = L(t)$ migrates to the left (Figure 3).

Shrinkage factor model

The shrinkage factor f was assumed to have the temperature dependence illustrated in Figure 2. This model is consistent with Hung's[10] work, which showed that muscle shrinkage depends primarily on temperature level, rather than on the time of exposure to that temperature level. The $f = 1$ limit represents the state of zero shrinkage at room temperature ($\theta = 0$). The shrinking does not continue indefinitely as the temperature increases. It stops at $f = f_\infty$, when the temperature reaches the level represented by the dimensionless θ_2 on the abscissa. The shrinking begins when the temperature exceeds θ_1, and the decrease of f from $f(\theta_1) = 1$ to $f(\theta_2) = f_\infty$ is assumed linear.

The dimensionless constants $(f_\infty, \theta_1, \theta_2)$ for the model of Figure 2 must be determined empirically; however, they are independent of the size of the cut of meat and the method of cooking. By using transmission electron microscopy, Hung[10] found that there are two stages in the shrinking of beef sarcomeres (sarcomeres are units of the myofibril, which make up muscle fibers). In the first stage, the sarcomeres shrink from approximately 2.5–2.05 μm. This first shrinkage is completed at fairly low temperatures and is not related to (accompanied by) weight loss. The second stage begins at $T_1 \cong 70°C$ and ends at $T_2 \cong 90°C$, while the sarcomeres shrink from 2.05–1.55 μm. Hung found that this second shrinkage is accompanied by weight loss, as discussed previously.

For the final, long-time value of the shrinkage factor f_∞ we used the values 0.7 and, later, 0.6, which cover the range of our own observations of steaks cooked "well done." In the case of a cut of meat initially at $T_0 = 25°C$ and cooked in an oven heated to $T_\infty = 163°C$ (325°F), the dimensionless "transition" temperatures marked on the abscissa of Figure 2 have

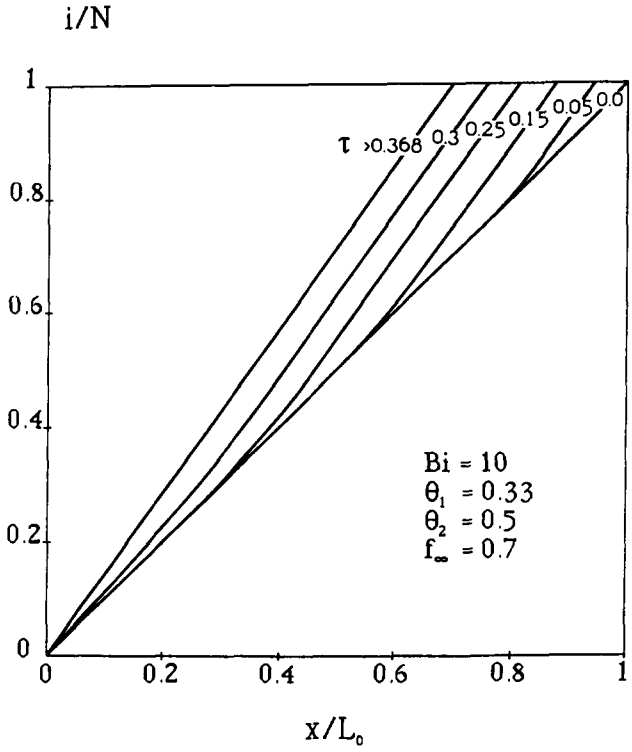

Figure 4 The evolution of the shrinking curve (Bi = 10, $\theta_1 = 0.33$, $\theta_2 = 0.5$, $f_\infty = 0.7$)

the values $\theta_1 = 0.33$ and $\theta_2 = 0.47$. Since T_0 and, especially, T_∞ can change from one application to another, the results exhibited in the next section cover the range $\theta_1 = 0.2$–0.33 and $\theta_2 = 0.4$–0.6.

Temperature history and cooking time

The results of this study are presented in Figures 4–6. To start with, Figure 4 confirms all the features of the shrinkage distribution curves anticipated in Figure 2. The curve of i/N *versus* x/L_0 deviates from the straight diagonal line as the time increases and as deeper strata of meat begin to shrink. In the case (Bi, θ_1, θ_2, f_∞) for which Figure 4 was constructed, the shrinking effect penetrates all the way to the midplane ($x = 0$) when the dimensionless time τ exceeds approximately 0.3.

Another interesting observation is that at intermediate times (e.g., $\tau = 0.15$) each curve in Figure 4 is straight both to the left and to the right of a relatively narrow "knee" region. To the left, i.e., toward the slab midplane, the slope of the line is 1/1, indicating that the inner strata have not experienced any shrinkage yet. To the right of the knee, the slope of the straight line is larger, $1/f_\infty$, meaning that the outer strata have all shrunk to their smallest size (or that the temperature of these strata has risen above θ_2, Figure 3). In conclusion, the only region in which the meat is shrinking is indicated by the curved knee. Since this active region is quite narrow—about 10 percent of the half-thickness L_0—the actual function $f(\theta)$ chosen between θ_1 and θ_2 (linear in Figure 3) does not have a significant impact on the results of this study.

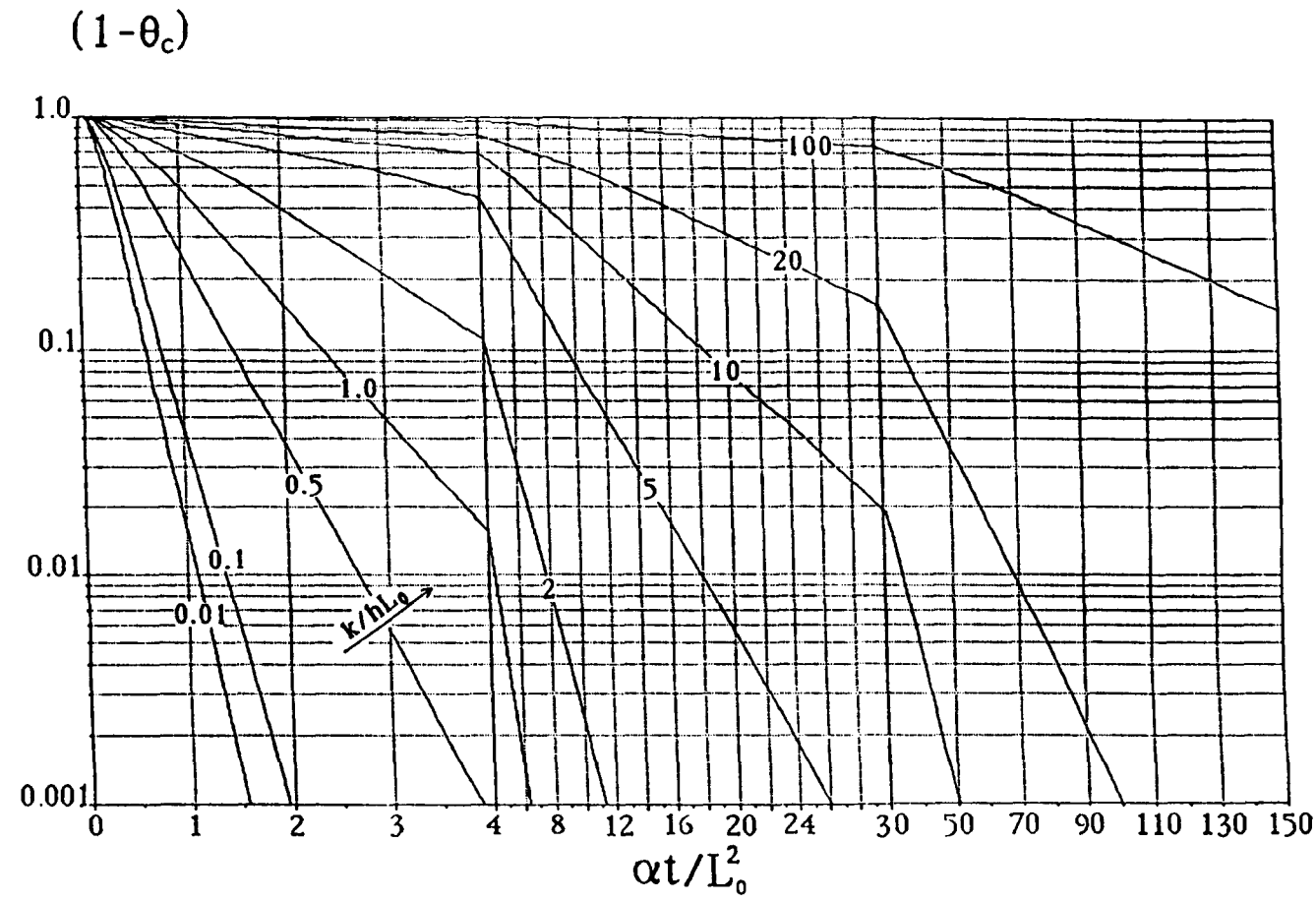

Figure 5 The temperature history in the midplane ($\theta_1 = 0.33$, $\theta_2 = 0.5$, $f_\infty = 0.7$)

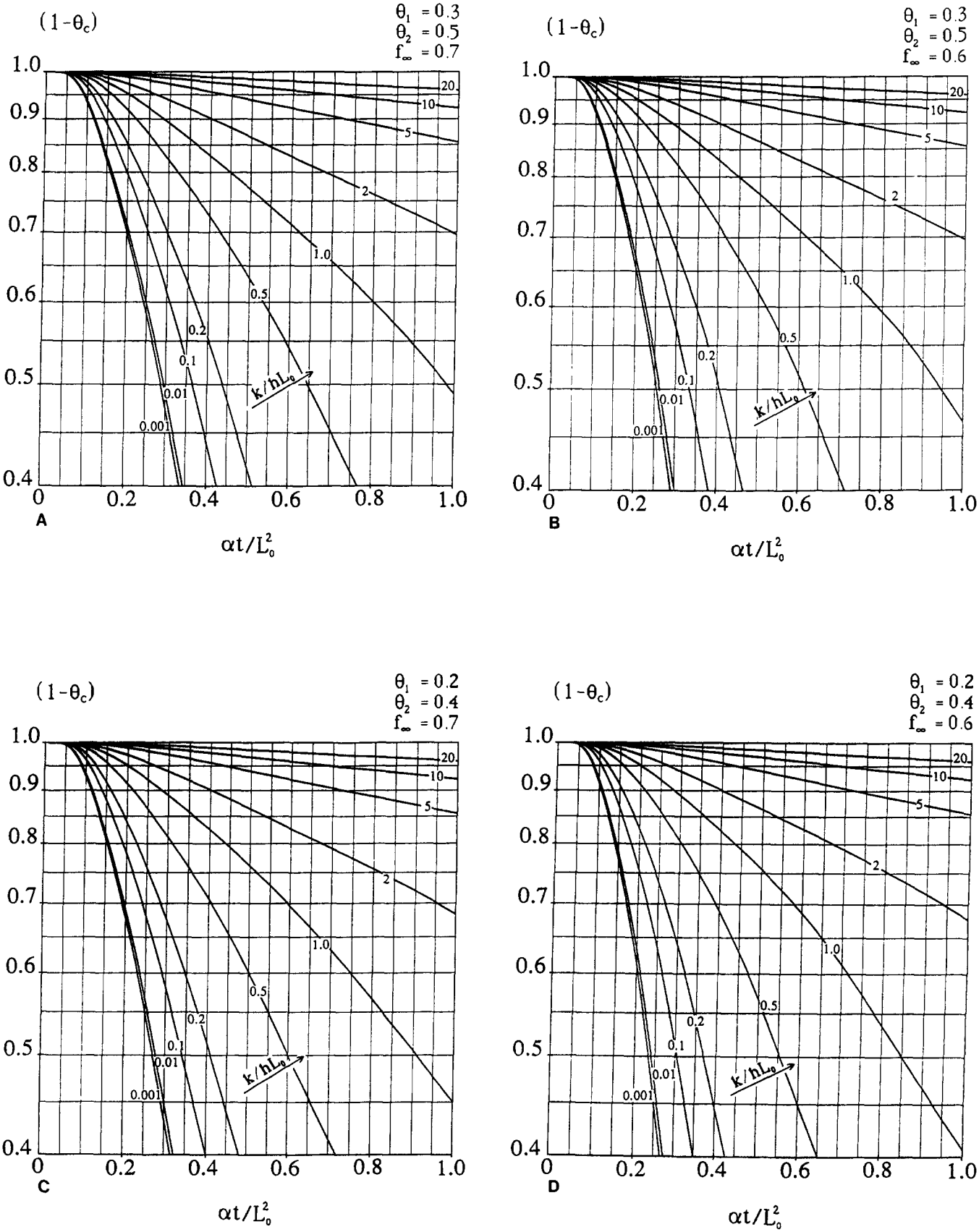

Figure 6 Charts for the temperature history in the midplane of a shrinking slab

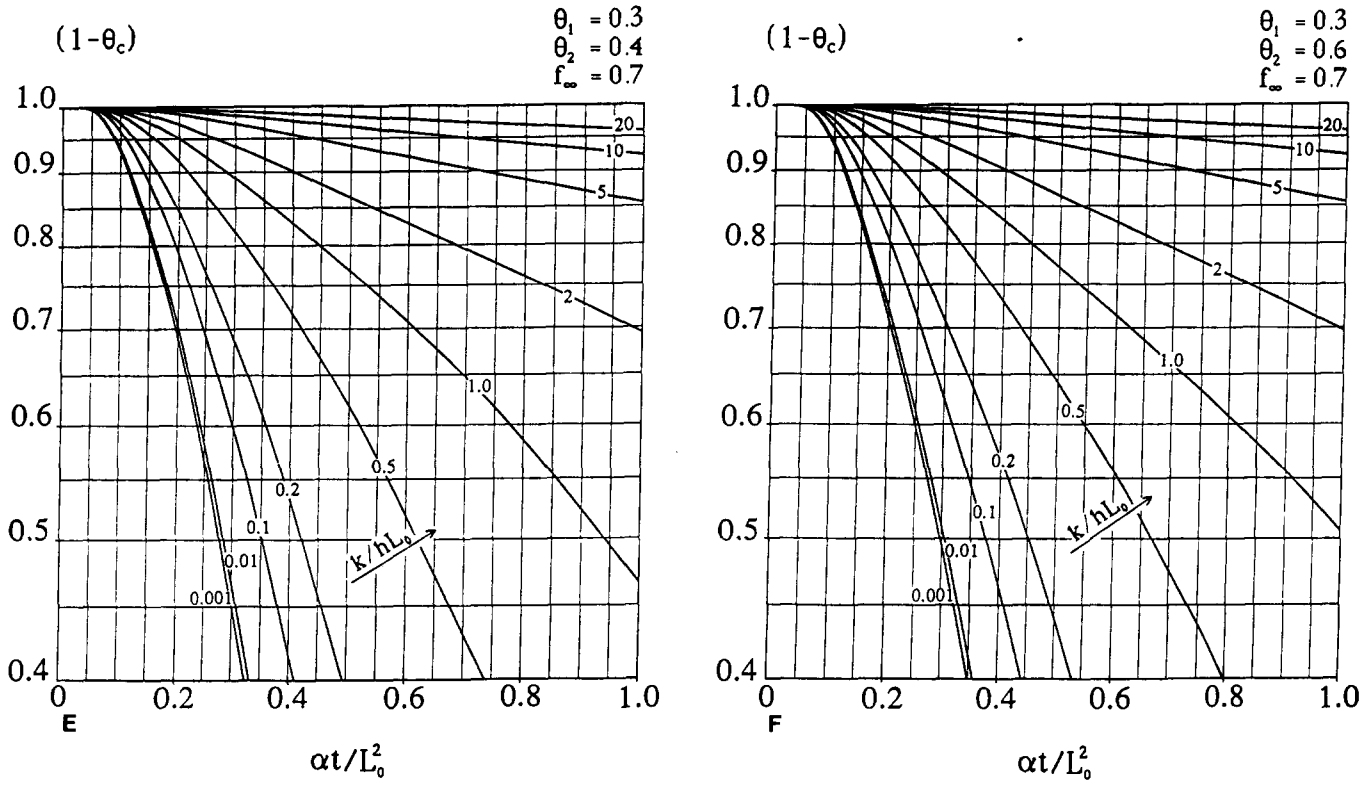

Figure 6 continued

A key issue in the cooking of meat is the calculation of the required cooking time. Since the final degree of cooking (rare, medium, well done) is dictated by the temperature reached in the center of the cut of meat, it is important to know how the midplane temperature ($\theta = \theta_c$, at $x = 0$) increases with time, and how it is affected by the oven conditions (T_∞, h) and the size of the piece of meat (L_0). This information is presented beginning with Figure 5, which has the same features as the classical Heisler charts found in all heat transfer textbooks. In the case of meat cooking, the only relevant portion of this chart is the upper decade, where $0.1 < (1 - \theta_c) < 1$, because proper cooking requires only moderate temperature rises in the midplane. For example, beef is well done when its center temperature reaches approximately 82°C (or 180°F, Roberson and Roberson[15]), and this would correspond to a $(1 - \theta_c)$ value of only 0.59 if $T_\infty = 163$°C and $T_0 = 25$°C. This is why the ordinate in Figures 6a–f has been blown up to cover only the range $0.4 < (1 - \theta_c) < 1$.

The numerical procedure for estimating the required cooking time is illustrated by the following example. Consider the cooking of a 4-cm thick beefsteak in an oven at $T_\infty = 149$°C (300°F). The initial temperature of the steak is $T_0 = 25$°C. The center of the steak is to be cooked well done, $T_c = 82$°C (180°F), and this translates into a dimensionless $\theta_c = 0.46$, and $(1 - \theta_c) = 0.54$.

The cooking time can be read off one of the charts assembled in Figure 6. Note first that the transition temperatures for beef ($T_1 = 70$°C, $T_2 = 90$°C) have the dimensionless counterparts $\theta_1 = 0.36$ and $\theta_2 = 0.52$. The chart that comes closest to representing this case is Figure 6a. The reported value of the effective heat transfer coefficient (combined convection and radiation) in a convection oven varies from 18.5 W/m²°C in Burfoot and James[7] to 90 W/m²°C in Skjöldebrand.[1] In this example we set $h = 100$ W/m²°C as the representative order of magnitude of the effective heat transfer coefficient. This value and the thermal conductivity of lean beef (0.4 W/m°C) lead to an inverse Biot number k/hL_0 equal to 0.2. From Figure 6a we conclude that $\alpha t/L_0^2 \cong 0.41$, and, since for beef $\alpha = 1.25 \times 10^{-7}$ m²/s,[16] the actual time is $t \cong 21.9$ minutes.

One interesting aspect of this time estimate is that if we were to neglect the shrinkage effect entirely (i.e., if we would use the Heisler chart), we would obtain $t \cong 25.6$ minutes. Although at first glance the difference of 3.7 minutes between these two estimates does not seem great, it is actually large from the point or view of not overcooking the steak, or when trying to cook the steak rare as opposed to well done. For example, if we return to the present model (Figure 6a) and assume that the center of the steak is to be cooked rare, $T_c = 60$°C (140°F), we find that the required cooking time is $t \cong 15.5$ minutes. We see now that the same steak would be well done only 6.4 minutes later.

This numerical example has been extended in Figure 7 to a common range of meat-slab half-thicknesses L_0 and oven temperatures T_∞. Figure 7a shows the cooking time calculated by taking the effect of meat shrinking into account, while Figure 7b shows the base estimate in which the meat shrinking effect is neglected. Taken together, Figures 7a and b show that the cooking time is shortened by the effect of meat shrinking. In both figures, the cooking time increases with the half-thickness L_0, and decreases with the oven temperature T_∞.

The effect of the meat shrinking parameters θ_1, θ_2, f_∞ can be seen by comparing the six temperature charts of Figure 6 with the corresponding chart for a conduction process in which the shrinkage is absent (Figure 8). The information found in Figure 8 is available also in Heisler's[14] chart. This comparison shows that lower values of θ_1, θ_2, and f_∞ lead to steeper $(1 - \theta_c)$ curves, i.e., to shorter cooking times. It is worth noting that the changes in θ_1 and f_∞ have a stronger impact on the cooking time than the changes in θ_2. This is fortunate, because θ_1 and f_∞ are easier to measure experimentally than θ_2.

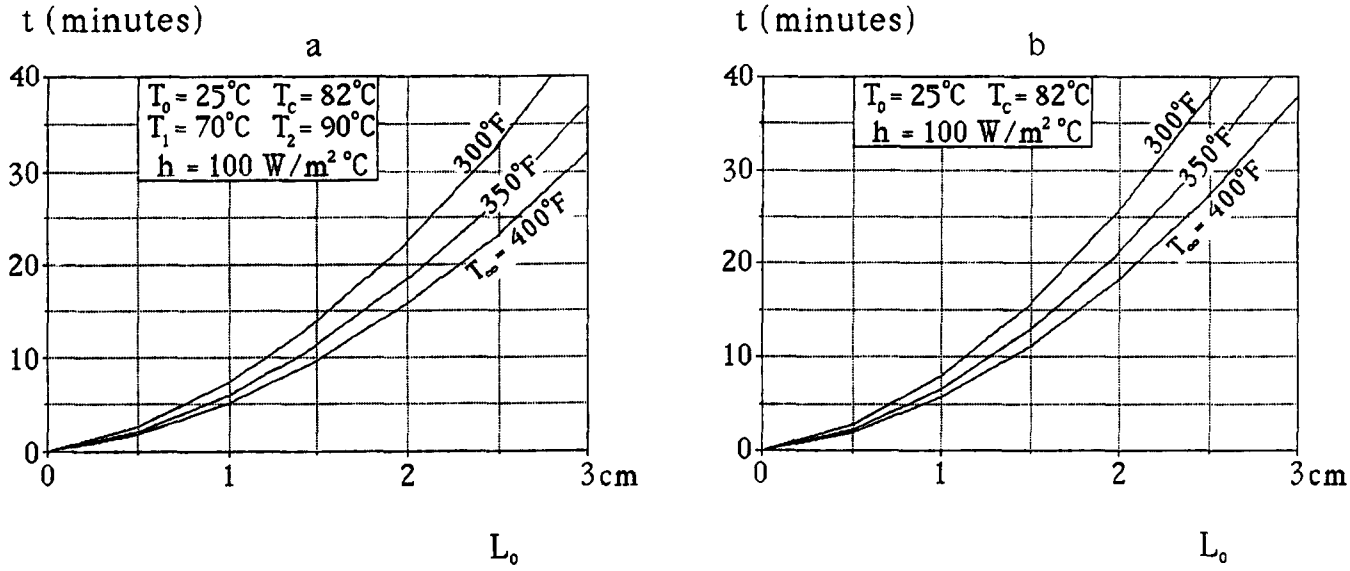

Figure 7 Numerical example: the cooking times for well done beef steak. (a) Model with meat shrinking, Figure 1; (b) model without shrinking[14]

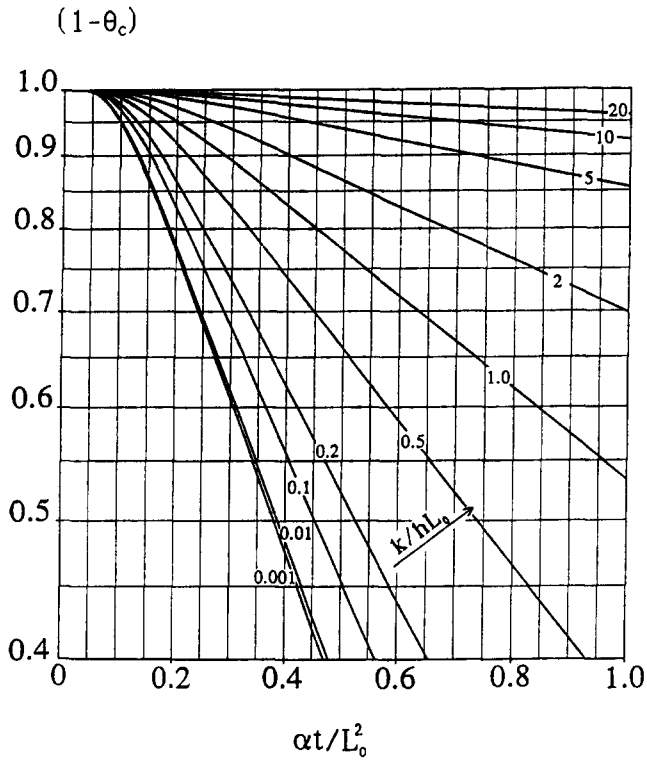

Figure 8 The temperature history in the midplane of a slab that does not shrink

In dimensionless terms, the same comparison between Figure 6 (with shrinkage) and Figure 8 (without shrinkage) shows that the $(1-\theta_c)$ curves are relatively steeper at lower k/hL_0 values. This means that the effect of meat shrinking gains in importance as the Biot number increases, i.e., as one contemplates faster cooking methods (e.g., the methods of the fast-food industry: broiling, frying, and deep-frying).

Conclusion

The objective of this work was to examine a new aspect of the process of meat cooking, namely, the effect of the shrinking of the meat as the temperature rises. The overall shrinkage, or the movement of the surfaces toward the center of the piece of meat, is due to a process that is distributed volumetrically and tied to the local temperature history of each layer of meat.

Means for anticipating the temperature history in the center of the piece of meat and the cooking time required to reach a certain temperature were determined numerically and reported in the form of generalized (dimensionless) charts (Figures 6a–f). Although similar to the classical Heisler charts for time-dependent conduction in a constant-volume slab, these new charts predict cooking times that are signifificantly shorter than the corresponding estimates based on Heisler's charts. The effect of the shrinking process then is to accelerate the cooking of the innermost region of the piece of meat.

Acknowledgement

This work was supported in part by a Biomedical Research Support Grant from the National Institutes of Health.

References

1 Skjöldebrand, C. Convection oven frying: heat and mass transfer between air and product. *Journal of Food Science*, 1980, **45**, 1354–1362

2 Holtz, E., and Skjöldebrand, B. Modeling the baking process of meat products using convection ovens. *Thermal Processing and Quality of Foods*, P. Zeuthen, et al., eds. Elsevier, London and New York, 1984, 329–338

3 Holtz, E., and Skjöldebrand, C. Simulation of the temperature of a meat loaf during the cooking process. *Journal of Food Engineering*, 1986, **5**, 109–121

4 Chau, K. V., and Snyder, G. V. Mathematical model for temperature distribution of thermally processed shrimp. *Trans. ASAE*, 1988, **31**, 608–612

5 Bengtsson, N., Jakobsson, B., and Dagerskog, M. Cooking of beef by oven roasting: a study of heat and mass transfer. *Journal of Food Science*, 1976, **41**, 1047–1053

6 Dagerskog, M. Pan frying of meat patties I and II. *Lebensm.-Wiss. u.-Technol.*, 1979, **12**, 217–230

7 Burfoot, D., and James, S. J. Problems in mathematically modelling the cooking of a joint of meat. *Thermal Processing and Quality of Foods*, P. Zeuther, et al., eds. Elsevier, London and New York, 1984, 467–472

8 Burfoot, D., and James, J. The effect of spatial variations of heat transfer coefficient on meat processing times. *Journal of Food Engineering*, 1988, **7**, 41–61

9 Hamm, R. Heating of muscle systems. *The Physiology and Biochemistry of Muscle as a Food*, E. J. Briskey et al., eds. University of Wisconsin Press, Madison, Milwaukee, and London, 1966, 363–387

10 Hung, C. C. Water migration and structural transformation of oven cooked meat. Ph.D. Thesis, University of Minnesota, MN, USA, 1980

11 Godsalve, E. W., Davis, E. A., Gordon, J., and Davis, H. T. Water loss rates and temperature profiles of dry cooked bovine muscle. *Journal of Food Science*, 1977, **42**, 1038–1045

12 Godsalve, E. W. Heat and mass transfer in cooking meat. Ph.D. Thesis, University of Minnesota, MN, USA, 1976

13 McGee, H. *On Food and Cooking*. Scribners, New York, 1984, 105–112

14 Heisler, M. P. Temperature charts for induction and constant-temperature heating. *Trans. ASME*, 1947, **69**, 227–236

15 Roberson, J. and Roberson, M. *The Meat Cookbook*. Collier, New York, 1966, 44

16 Morley, M. J. Thermal properties of meat: tabulated data. Special Report No. 1. Meat Research Institute, Langford, Bristol, UK, 1972